Flux tubes in the SU(3) vacuum: London penetration depth and coherence length

Paolo Cea[*]

Dipartimento di Fisica dell'Università di Bari, I-70126 Bari, Italy and INFN, Sezione di Bari, I-70126 Bari, Italy

Leonardo Cosmai[†]

INFN, Sezione di Bari, I-70126 Bari, Italy

Francesca Cuteri[‡] and Alessandro Papa[§]

Dipartimento di Fisica dell'Università della Calabria, I-87036 Arcavacata di Rende, Cosenza, Italy and INFN, Gruppo collegato di Cosenza, I-87036 Arcavacata di Rende, Cosenza, Italy

Within the dual superconductor scenario for the QCD confining vacuum, the chromoelectric field generated by a static $q\bar{q}$ pair can be fitted by a function derived, by dual analogy, from a simple variational model for the magnitude of the normalized order parameter of an isolated Abrikosov vortex. Previous results for the SU(3) vacuum are revisited, but here the transverse chromoelectric field is measured by means of the connected correlator of two Polyakov loops and, in order to reduce noise, the smearing procedure is used instead of cooling. The penetration and coherence lengths of the flux tube are then extracted from the fit and compared with previous results.

I. INTRODUCTION

It is well established that in the QCD vacuum at zero temperature two static color charges give rise to chromoelectric flux tubes signalling color confinement [1,2]. As a matter of fact, Monte Carlo simulations of lattice QCD allow a nonperturbative study of tube-like structures that emerge by analyzing the chromoelectric fields between static quarks [3–19].

This suggests to us a direct physical analogy between the QCD vacuum and an electric superconductor. Indeed, 't Hooft [20] and Mandelstam [21] conjectured a long time ago that the vacuum of QCD could be modeled as a coherent state of color magnetic monopoles, namely as a dual superconductor [22]. In the dual superconductor model of the QCD vacuum the condensation of color magnetic monopoles is analogous to the formation of Cooper pairs in the BCS theory of superconductivity. Even though the dynamical formation of color magnetic monopoles is not explained by the 't Hooft construction, there are convincing lattice evidences [23–31] for the color magnetic condensation in the QCD vacuum. It should be remarked, however, that the color magnetic monopole condensation in the confinement mode of QCD could be a consequence, rather than the origin, of the mechanism of color confinement [32]. Notwithstanding, the dual superconductivity picture of the

QCD vacuum remains at least a useful phenomenological frame to interpret the vacuum dynamics.

In previous studies [12–16,33] color flux tubes made up of the chromoelectric field directed along the line joining a static quark-antiquark pair have been investigated for both SU(2) and SU(3) gauge theories. In particular, to explore on the lattice the field configurations produced by a static quark-antiquark pair, the following connected correlation function [7,8,34,35] was used:

$$\rho_W^{\text{conn}} = \frac{\langle \text{tr}(WLU_PL^\dagger)\rangle}{\langle \text{tr}(W)\rangle} - \frac{1}{N}\frac{\langle \text{tr}(U_P)\text{tr}(W)\rangle}{\langle \text{tr}(W)\rangle}, \quad (1)$$

where $U_P = U_{\mu\nu}(x)$ is the plaquette in the (μ,ν) plane, connected to the Wilson loop W by a Schwinger line, L, and N is the number of colors (see Fig. 1 in Refs. [16,33]). The correlation function defined in Eq. (1) measures the field strength, since in the naive continuum limit [8]

$$\rho_W^{\text{conn}} \xrightarrow{a\to 0} a^2 g[\langle F_{\mu\nu}\rangle_{q\bar{q}} - \langle F_{\mu\nu}\rangle_0], \quad (2)$$

where $\langle\rangle_{q\bar{q}}$ denotes the average in the presence of a static $q\bar{q}$ pair and $\langle\rangle_0$ is the vacuum average. Accordingly, we are led to define the quark-antiquark field strength tensor as

$$F_{\mu\nu}(x) = \sqrt{\frac{\beta}{2N}}\,\rho_W^{\text{conn}}(x). \quad (3)$$

As is well known from the usual electric superconductivity, tube-like structures arise as a solution of the

[*]paolo.cea@ba.infn.it
[†]leonardo.cosmai@ba.infn.it
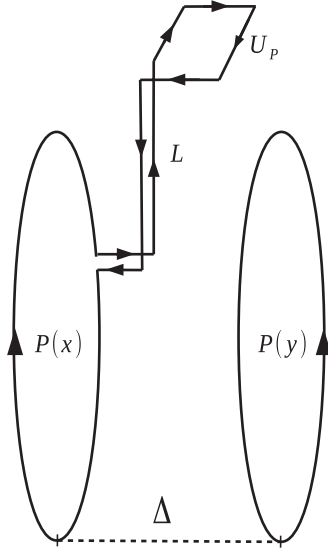[‡]francesca.cuteri@cs.infn.it
[§]papa@cs.infn.it

FIG. 1.   The connected correlator given in Eq. (10) between the plaquette U_P and the Polyakov loops (subtraction in ρ_P^{conn} is not explicitly drawn).

Ginzburg-Landau equations [36]. Similar solutions were found by Nielsen and Olesen [37] in the case of the Abelian Higgs model, namely the relativistic version of the Ginzburg-Landau theory. In the dual superconductor model of the QCD vacuum, the formation of the chromoelectric flux tube can be interpreted as the dual Meissner effect. In this context the transverse shape of the longitudinal chromoelectric field E_l should resemble the dual version of the Abrikosov vortex field distribution. Therefore, the proposal was advanced [10,12–16] to fit the transverse shape of the longitudinal chromoelectric field according to

$$E_l(x_t) = \frac{\Phi}{2\pi}\mu^2 K_0(\mu x_t), \qquad x_t > 0, \qquad (4)$$

where K_n is the modified Bessel function of the order n, Φ is the external flux, and $\lambda = 1/\mu$ is the London penetration length. Note that Eq. (4) is valid as long as $\lambda \gg \xi$, where ξ is the coherence length of a type-II superconductor, which measures the coherence of the magnetic monopole condensate (the dual version of the Cooper condensate). However, several numerical studies [9,38–47] in both SU(2) and SU(3) lattice gauge theories have shown that the confining vacuum behaves much like an effective dual superconductor, which lies on the borderline between a type-I and a type-II superconductor. If this is the case, Eq. (4) is no longer adequate to account for the transverse structure of the longitudinal chromoelectric field. In fact, in Ref. [48] it has been suggested that lattice data for chromoelectric flux tubes can be analyzed by exploiting the results presented in Ref. [49], where, from the assumption of a simple variational model for the magnitude of the normalized order parameter of an isolated vortex, an

analytic expression is derived for the magnetic field and supercurrent density that solves the Ampere's law and the Ginzburg-Landau equations. As a consequence, the transverse distribution of the chromoelectric flux tube can be described according to [48]

$$E_l(x_t) = \frac{\phi}{2\pi}\frac{1}{\lambda\xi_v}\frac{K_0(R/\lambda)}{K_1(\xi_v/\lambda)}, \qquad (5)$$

where

$$R = \sqrt{x_t^2 + \xi_v^2}, \qquad (6)$$

and ξ_v is a variational core-radius parameter. Equation (5) can be rewritten as

$$E_l(x_t) = \frac{\phi}{2\pi}\frac{\mu^2}{\alpha}\frac{K_0[(\mu^2 x_t^2 + \alpha^2)^{1/2}]}{K_1[\alpha]}, \qquad (7)$$

with

$$\mu = \frac{1}{\lambda}, \qquad \frac{1}{\alpha} = \frac{\lambda}{\xi_v}. \qquad (8)$$

By fitting Eq. (7) to flux-tube data, one can obtain both the penetration length λ and the ratio of the penetration length to the variational core-radius parameter λ/ξ_v. Moreover, the Ginzburg-Landau κ parameter can be obtained by

$$\kappa = \frac{\lambda}{\xi} = \frac{\sqrt{2}}{\alpha}[1 - K_0^2(\alpha)/K_1^2(\alpha)]^{1/2}. \qquad (9)$$

Finally, the coherence length ξ can be obtained by combining Eqs. (8) and (9).

Our aim is to extend previous studies of the structure of flux tubes performed at zero temperature to the case of SU(3) pure gauge theory at finite temperatures. In fact, the nonperturbative study of the chromoelectric flux tubes generated by static color sources at finite temperature is directly relevant to clarify the formation of $c\bar{c}$ and $b\bar{b}$ bound states in heavy ion collisions at high energies. To implement this program, however, we cannot employ the Wilson loop operator in the connected correlation in Eq. (1). This problem can be easily overcome if we replace in Eq. (1) the Wilson loop with two Polyakov lines. In addition, we need to replace the cooling mechanism previously used to enhance the signal-to-noise ratio. Indeed, cooling is a well established method for locally suppressing quantum fluctuations in gauge field configurations. However, at finite temperatures the cooling procedure tends to also suppress thermal fluctuations. Fortunately, there is an alternative, yet somewhat related, approach that is the application of APE smearing [50,51] to the gauge field configurations. This approach also leads to the desirable effect of suppressing lattice artifacts at the scale of the cutoff without affecting the thermal

fluctuations. Moreover, this procedure can be iterated many times to obtain smoother and smoother gauge field configurations. Obviously, we must preliminarily check that this method gives results which are consistent with previous studies obtained with Wilson loops and cooling. In this paper we present numerical results on the chromoelectric flux tubes generated by static color sources in SU(3) pure gauge theory at zero temperature obtained with connected correlations built with Polyakov lines and smeared gauge links.

The plan of the paper is as follows. The connected correlation built with Polyakov lines, used in this paper, is reported in Sec. II. In Sec. III we present our numerical results for SU(3). In Sec. IV we check the scaling of the penetration and coherence lengths and compare with previous studies. Finally, in Sec. V we summarize our results and present our conclusions.

II. FLUX TUBES ON THE LATTICE

According to our previous discussion, we shall consider the following connected correlations (depicted in Fig. 1):

$$\rho_P^{\text{conn}} = \frac{\langle \text{tr}(P(x) L U_P L^\dagger) \text{tr} P(y) \rangle}{\langle \text{tr}(P(x)) \text{tr}(P(y)) \rangle}$$
$$- \frac{1}{3} \frac{\langle \text{tr}(P(x)) \text{tr}(P(y)) \text{tr}(U_P) \rangle}{\langle \text{tr}(P(x)) \text{tr}(P(y)) \rangle}, \qquad (10)$$

where the two Polyakov lines separated by a distance Δ replace the Wilson loop in Eq. (1). Taking into account Eqs. (2) and (3), we may define the field strength tensor as

$$F_{\mu\nu}(x) = \sqrt{\frac{\beta}{6}} \, \rho_P^{\text{conn}}(x). \qquad (11)$$

A detailed derivation of Eq. (11), together with the discussion of its physical interpretation, can be found in Ref. [52]. We performed numerical simulations on 20^4 lattices using the Wilson action with periodic boundary conditions and the Cabibbo-Marinari algorithm [53] combined with overrelaxation on SU(2) subgroups. We considered Polyakov lines separated by $\Delta = 4a, 6a, 8a$ (where a is the lattice spacing) for four different values of the gauge coupling β in the range $5.9 \div 6.1$. In order to reduce the autocorrelation time, measurements were taken after 10 updatings. The error analysis was performed by the jackknife method over bins at different blocking levels. To reduce statistical errors we employed the smearing procedure as described in Ref. [50,51], with the smearing parameter $\epsilon = 0.5$. We checked that numerical results are stable, within the statistical uncertainties, under small variations of the parameter ϵ.

As in previous studies, we confirm that the flux tube is almost completely formed by the longitudinal chromoelectric field E_l, which is constant along the flux axis and
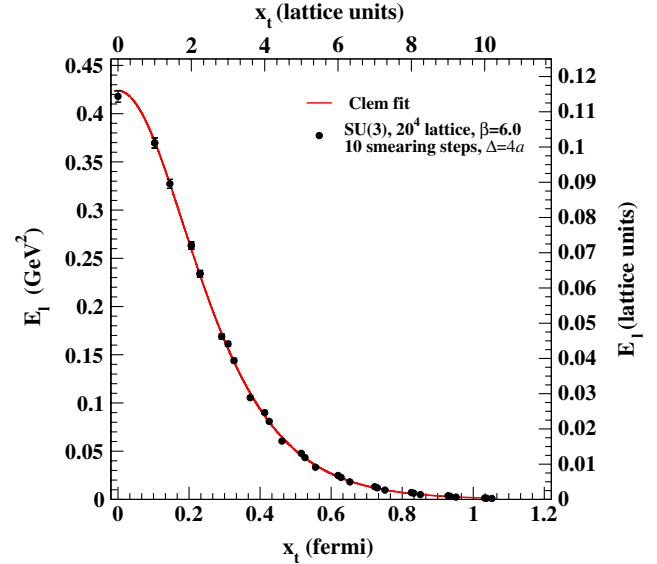

FIG. 2 (color online). The longitudinal chromoelectric field E_l versus x_t, in lattice units and in physical units, at $\beta = 6.0$ and for $\Delta = 4a$, after 10 smearing steps. Intermediate distances are included. The full line is the best fit using Eq. (7). The procedure to fix the physical scale is explained in Sec. IV.

decreases rapidly in the transverse direction x_t. In Fig. 2 we display the transverse distribution of the longitudinal chromoelectric field, measured at the middle point (labeled by $x_t = 0$) of the line connecting the static color sources and at various distances $x_t > 0$ from this point along one of the transverse spatial directions. To check rotational invariance, we also considered points calculated at noninteger distances. We fitted our data to Eq. (7). The results are displayed in Fig. 2, where the full line is the curve fitting of the data. As is evident, even in the present case Eq. (7) is able to accurately reproduce the transverse distribution of the longitudinal chromoelectric field. We also tried to restrict the fit only to points at integer distances and obtained consistent values for the fit parameters. The unique observable effect was a drastic reduction of the reduced chi-square, χ_r^2. Therefore, to save CPU time, we decided to perform measurements of the connected correlations, Eq. (10), for integer transverse distances only.

III. NUMERICAL DATA

We measured the connected correlator, Eq. (10), for integer transverse distances, x_t, at $\beta = 5.9, 6.0, 6.05, 6.1$. To reduce statistical fluctuations in gauge field configurations, we performed measurements after several smearing steps. For each smearing, we fitted our data for the transverse shape of the longitudinal chromoelectric field to Eq. (7). As a result, we obtained the fit parameters for different smearing steps. This allowed us to check the dependence of these parameters on the number of smearing steps. In fact, we found a well defined plateau in the

TABLE I. Summary of the fit values at $\beta = 6.0$ for $\Delta = 6a$. The last column gives the reduced chi-square.

Smearing	ϕ	μ	λ/ξ_v	κ	χ_r^2
16	6.191(141)	0.621(79)	0.309(95)	0.213(91)	0.018
18	6.218(125)	0.622(76)	0.287(82)	0.192(77)	0.011
20	6.227(109)	0.617(68)	0.277(72)	0.183(66)	0.010
22	6.222(98)	0.608(61)	0.271(64)	0.178(58)	0.010
24	6.207(88)	0.597(55)	0.269(58)	0.176(53)	0.011
26	6.184(81)	0.587(50)	0.269(54)	0.175(49)	0.011
28	6.155(75)	0.576(47)	0.269(51)	0.176(46)	0.011
30	6.122(70)	0.566(44)	0.270(48)	0.176(44)	0.010
32	6.087(66)	0.557(41)	0.271(46)	0.177(42)	0.009
34	6.049(63)	0.549(39)	0.271(45)	0.178(41)	0.008
36	6.011(60)	0.541(37)	0.272(43)	0.179(40)	0.007
38	5.973(58)	0.534(36)	0.273(42)	0.179(39)	0.005
40	5.935(56)	0.527(35)	0.274(42)	0.180(38)	0.004
42	5.897(54)	0.521(34)	0.274(41)	0.180(37)	0.003
44	5.859(53)	0.515(33)	0.275(40)	0.181(37)	0.003
46	5.822(51)	0.510(32)	0.275(40)	0.181(37)	0.002
48	5.786(50)	0.505(31)	0.276(39)	0.182(36)	0.002
50	5.751(49)	0.500(31)	0.277(39)	0.182(36)	0.001

extracted parameter values versus the smearing steps. To appreciate this point we report in Table I the values of the fit parameters for smearing steps ranging from 16 up to 50. The parameters refer to the fit of the field strength tensor, corresponding to the connected correlator Eq. (10) at $\beta = 6.0$ and $\Delta = 6a$. Note that the parameters ϕ, μ, and λ/ξ_v are obtained by the fitting procedure, while the Ginzburg-Landau parameter κ is evaluated by means of Eq. (9). We looked also for contamination effects on the longitudinal chromoelectric field due to the presence of the static color sources. To do this, we varied the distance Δ between the Polyakov lines: we found that the fitting

parameters μ and λ/ξ_v for $\Delta = 4a$ were systematically higher than for $\Delta = 6a, 8a$. On the other hand, we obtained parameters consistent within the statistical uncertainties for the distances $\Delta = 6a$ and $8a$. Since for $\Delta = 8a$ our estimate of the fitting parameters was affected by large statistical errors, we focused on the distance $\Delta = 6a$ as a good compromise between the absence of spurious contamination effects due to the static color sources and a reasonable signal-to-noise ratio.

In Figs. 3, 4, and 5 we display the fitting parameters ϕ, μ, and λ/ξ_v for different values of the gauge coupling β and
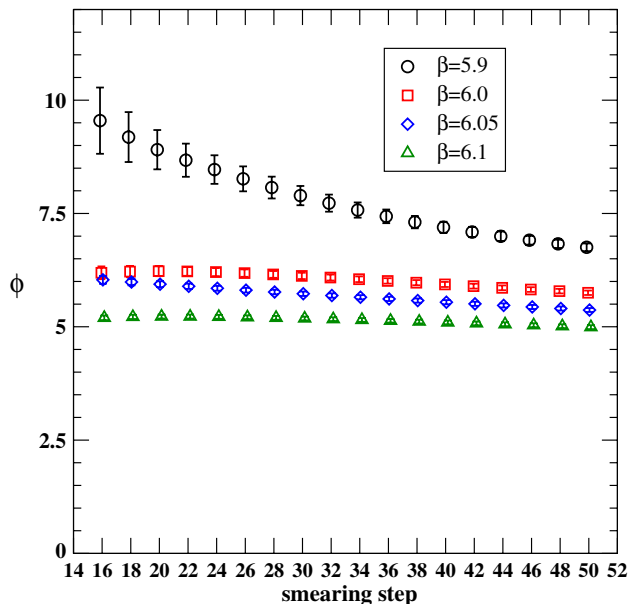
FIG. 3 (color online). ϕ versus the smearing step for $\Delta = 6a$.
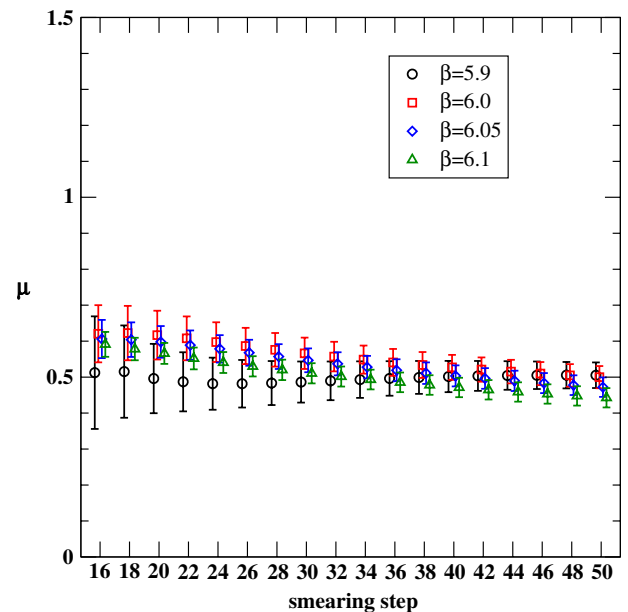
FIG. 4 (color online). μ versus the smearing step for $\Delta = 6a$. Here and in the following two figures data have been slightly shifted along the horizontal axis for the sake of readability.
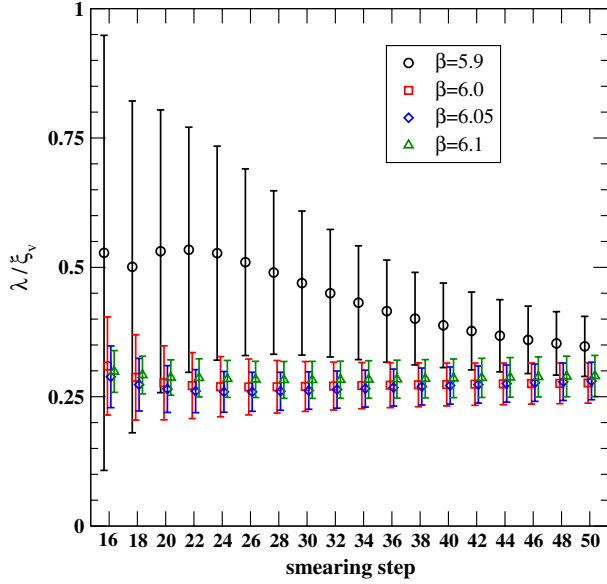
FIG. 5 (color online). λ/ξ_v versus the smearing step for $\Delta = 6a$.

the smearing step. We see, at least for $\beta \geq 6.0$, that our estimate for the fitting parameters seems to be reliable and independent of the number of smearing steps. The same holds also for the Ginzburg-Landau parameter κ (displayed in Fig. 6) as obtained from Eq. (9). As for $\beta = 5.9$, we observe a slower approach of the fitting parameters to a plateau, although this effect overcomes the statistical uncertainties only in the case of the parameter ϕ. A possible reason for this phenomenon could be the presence of lattice artifacts which need a larger number of smearing steps to be washed out and also spoil the continuum scaling, as will be confirmed in what follows.
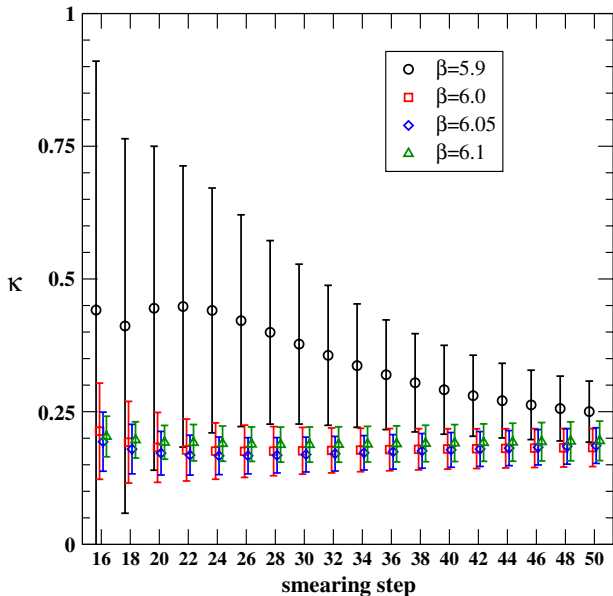
FIG. 6 (color online). κ versus the smearing step for $\Delta = 6a$.

IV. PENETRATION AND COHERENCE LENGTHS

Within our approach the shape of the longitudinal chromoelectric field is fully characterized by the London penetration depth, λ, and the coherence length, ξ. Thus, in view of phenomenological applications in hadron physics, it is important to estimate these lengths in physical units. First, we need to study the scaling of the plateau values of $a\mu$ with the string tension. For this purpose, we expressed these values of $a\mu$ in units of $\sqrt{\sigma}$, using the parametrization [54]

$$\sqrt{\sigma}(g) = f_{SU(3)}(g^2)[1 + 0.2731\hat{a}^2(g) - 0.01545\hat{a}^4(g)$$
$$+ 0.01975\hat{a}^6(g)]/0.01364,$$

$$\hat{a}(g) = \frac{f_{SU(3)}(g^2)}{f_{SU(3)}(g^2(\beta = 6))},$$

$$\beta = \frac{6}{g^2}, \qquad 5.6 \leq \beta \leq 6.5, \tag{12}$$

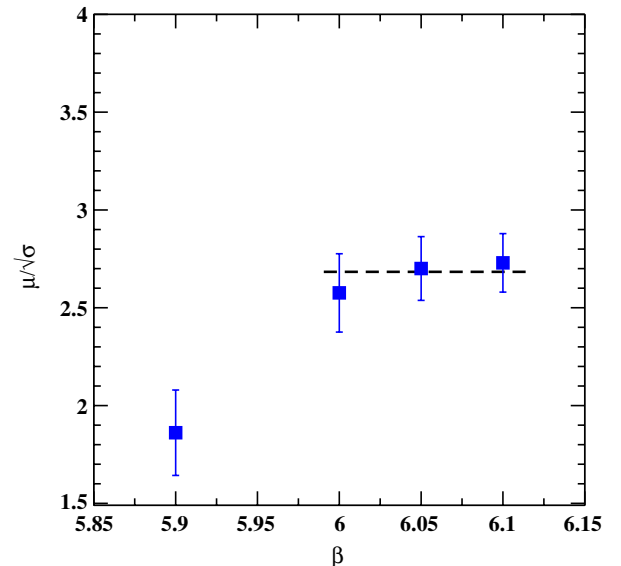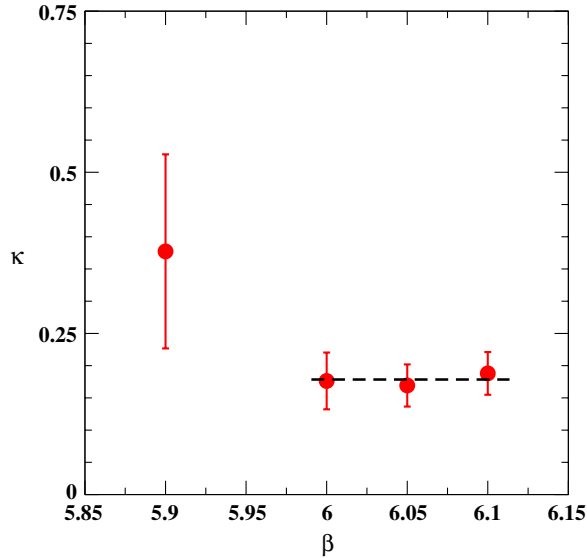where

$$f_{SU(3)}(g^2) = (b_0 g^2)^{-b_1/2b_0^2} \exp\left(-\frac{1}{2b_0 g^2}\right),$$

$$b_0 = \frac{11}{(4\pi)^2}, \qquad b_1 = \frac{102}{(4\pi)^4}. \tag{13}$$

In Fig. 7 we show the ratio $\mu/\sqrt{\sigma}$ for different values of the gauge coupling. We see that for $\beta \geq 6.0$, μ scales according to the string tension. Fitting the data in the scaling window with a constant, we get

$$\frac{\mu}{\sqrt{\sigma}} = 2.684(97). \tag{14}$$

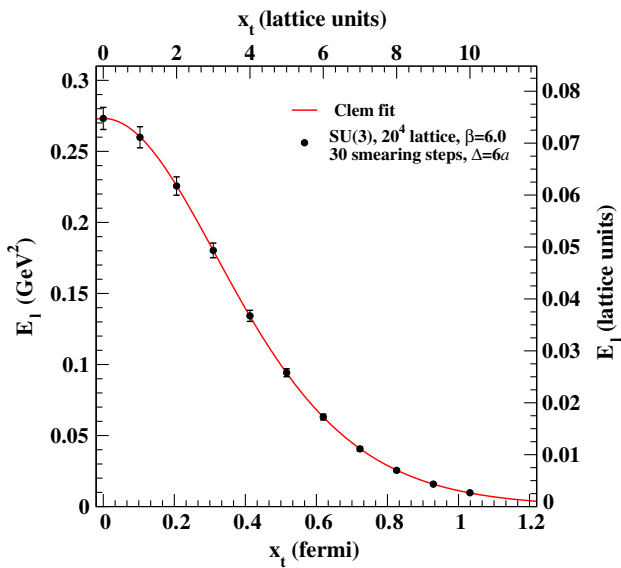FIG. 7 (color online). $\mu/\sqrt{\sigma}$ versus β for $\Delta = 6a$.

FIG. 8 (color online). κ versus β for $\Delta = 6a$.

Likewise, the dimensionless Ginzburg-Landau parameter κ scales in the same interval of β (see Fig. 8). Again, fitting with a constant gives

$$\kappa = 0.178(21). \tag{15}$$

It is reassuring to see that our determinations, Eqs. (14) and (15), are in good agreement with the values reported in Ref. [48], namely

$$\frac{\mu}{\sqrt{\sigma}} = 2.799(38), \qquad \kappa = 0.243(88), \tag{16}$$

FIG. 9 (color online).   Longitudinal chromoelectric field E_l versus x_t, in lattice units and in physical units, for $\Delta = 6a$ and after 30 smearing steps. The full line is the best fit using Eq. (7).

obtained using the connected correlator built with the Wilson loop, Eq. (1).

Assuming the standard value for the string tension, $\sqrt{\sigma} = 420$ MeV, from Eq. (14) we get

$$\lambda = \frac{1}{\mu} = 0.1750(63) \text{ fm.} \tag{17}$$

Combining Eqs. (17) and (15), we readily obtain

$$\xi = 0.983(121) \text{ fm.} \tag{18}$$

Finally, it is interesting to display the transverse structure of the longitudinal chromoelectric field produced by a static quark-antiquark pair in physical units; see Figs. 2 and 9.

V. SUMMARY AND CONCLUSIONS

In this paper we studied the chromoelectric field distribution between a static quark-antiquark pair in the confining vacuum of the SU(3) pure gauge theory.

Differently from our previous studies, we adopted here a connected correlator built with Polyakov lines rather than Wilson loops. This is a preliminary and necessary step towards the extension of this analysis to the case of nonzero temperature. Pushing forward the dual analogy with ordinary superconductivity and relying on a simple variational model for the magnitude of the normalized order parameter of an isolated vortex, we fitted the transverse behavior of the longitudinal chromoelectric field according to Eq. (7), which allowed us to get information on the penetration and coherence lengths. We observe that what we called "penetration length" could match the "intrinsic width" of the flux tube as defined in Ref. [55], where the adopted probe observable was the disconnected correlator of two Polyakov lines and a plaquette.

Our results are in good agreement with studies performed with the connected correlator with Wilson loop, and confirm that the SU(3) vacuum behaves as a type-I dual superconductor.

This conclusion is shared with Ref. [56], where the non-Abelian dual Meissner effect is investigated within the so-called "restricted field dominance." More recently, the same authors [57,58] presented some preliminary studies at nonzero temperature. Finally, we observe that our estimate of the London penetration length is in good agreement with the recent determination in Ref. [59], obtained using correlators of a plaquette with a Wilson loop, not connected by the Schwinger line, thus leading to the (more noisy) squared chromoelectric and chromomagnetic fields.

ACKNOWLEDGMENTS

[1] M. Bander, Phys. Rep. **75,** 205 (1981).

[2] J. Greensite, Prog. Part. Nucl. Phys. **51,** 1 (2003).

[3] M. Fukugita and T. Niuya, Phys. Lett. **132B,** 374 (1983).

[4] J. E. Kiskis and K. Sparks, Phys. Rev. D **30,** 1326 (1984).

[5] J. W. Flower and S. W. Otto, Phys. Lett. **160B,** 128 (1985).

[6] J. Wosiek and R. W. Haymaker, Phys. Rev. D **36,** 3297 (1987).

[7] A. Di Giacomo, M. Maggiore, and S. Olejnik, Phys. Lett. B **236,** 199 (1990).

[8] A. Di Giacomo, M. Maggiore, and S. Olejnik, Nucl. Phys. **B347,** 441 (1990).

[9] V. Singh, D. A. Browne, and R. W. Haymaker, Phys. Lett. B **306,** 115 (1993).

[10] P. Cea and L. Cosmai, Nucl. Phys. B, Proc. Suppl. **30,** 572 (1993).

[11] Y. Matsubara, S. Ejiri, and T. Suzuki, Nucl. Phys. B, Proc. Suppl. **34,** 176 (1994).

[12] P. Cea and L. Cosmai, Nuovo Cimento A **107,** 541 (1994).

[13] P. Cea and L. Cosmai, Nucl. Phys. B, Proc. Suppl. **34,** 219 (1994).

[14] P. Cea and L. Cosmai, Phys. Lett. B **349,** 343 (1995).

[15] P. Cea and L. Cosmai, Nucl. Phys. B, Proc. Suppl. **42,** 225 (1995).

[16] P. Cea and L. Cosmai, Phys. Rev. D **52,** 5152 (1995).

[17] G. S. Bali, K. Schilling, and C. Schlichter, Phys. Rev. D **51,** 5165 (1995).

[18] R. W. Haymaker and T. Matsuki, Phys. Rev. D **75,** 014501 (2007).

[19] A. D'Alessandro, M. D'Elia, and L. Tagliacozzo, Nucl. Phys. **B774,** 168 (2007).

[20] G. 't Hooft, in *High Energy Physics, EPS International Conference, Palermo, 1975,* edited by A. Zichichi (Editrice Compositori, Bologna, 1976), p. 1225.

[21] S. Mandelstam, Phys. Rep. **23,** 245 (1976).

[22] G. Ripka, Lect. Notes Phys. **639,** 1 (2004).

[23] H. Shiba and T. Suzuki, Phys. Lett. B **351,** 519 (1995).

[24] N. Arasaki, S. Ejiri, S.-i. Kitahara, Y. Matsubara, and T. Suzuki, Phys. Lett. B **395,** 275 (1997).

[25] P. Cea and L. Cosmai, Phys. Rev. D **62,** 094510 (2000).

[26] P. Cea and L. Cosmai, J. High Energy Phys. 11 (2001) 064.

[27] A. Di Giacomo, B. Lucini, L. Montesi, and G. Paffuti, Phys. Rev. D **61,** 034503 (2000).

[28] A. Di Giacomo, B. Lucini, L. Montesi, and G. Paffuti, Phys. Rev. D **61,** 034504 (2000).

[29] J. M. Carmona, M. D'Elia, A. Di Giacomo, B. Lucini, and G. Paffuti, Phys. Rev. D **64,** 114507 (2001).

[30] P. Cea, L. Cosmai, and M. D'Elia, J. High Energy Phys. 02 (2004) 018.

[31] A. D'Alessandro, M. D'Elia, and E. V. Shuryak, Phys. Rev. D **81,** 094501 (2010).

[32] G. 't Hooft, in Proceedings of the Large N_c QCD 2004, Trento, Italy, 2004 (World Scientific, Singapore, 2005).

[33] M. S. Cardaci, P. Cea, L. Cosmai, R. Falcone, and A. Papa, Phys. Rev. D **83,** 014502 (2011).

[34] D. S. Kuzmenko and Y. A. Simonov, Phys. Lett. B **494,** 81 (2000).

[35] A. Di Giacomo, H. G. Dosch, V. I. Shevchenko, and Y. A. Simonov, Phys. Rep. **372,** 319 (2002).

[36] A. A. Abrikosov, Sov. Phys. JETP **5,** 1174 (1957).

[37] H. B. Nielsen and P. Olesen, Nucl. Phys. **B61,** 45 (1973).

[38] T. Suzuki, Prog. Theor. Phys. **80,** 929 (1988).

[39] S. Maedan, Y. Matsubara, and T. Suzuki, Prog. Theor. Phys. **84,** 130 (1990).

[40] V. Singh, D. A. Browne, and R. W. Haymaker, Nucl. Phys. B, Proc. Suppl. **30,** 568 (1993).

[41] Y. Matsubara, S. Ejiri, and T. Suzuki, Nucl. Phys. B, Proc. Suppl. **34,** 176 (1994).

[42] C. Schlichter, G. S. Bali, and K. Schilling, Nucl. Phys. B, Proc. Suppl. **63,** 519 (1998).

[43] G. S. Bali, C. Schlichter, and K. Schilling, Prog. Theor. Phys. Suppl. **131,** 645 (1998).

[44] K. Schilling, G. Bali, and C. Schlichter, Nucl. Phys. B, Proc. Suppl. **73,** 638 (1999).

[45] F. Gubarev, E.-M. Ilgenfritz, M. Polikarpov, and T. Suzuki, Phys. Lett. B **468,** 134 (1999).

[46] Y. Koma, E.-M. Ilgenfritz, H. Toki, and T. Suzuki, Phys. Rev. D **64,** 011501 (2001).

[47] Y. Koma, M. Koma, E.-M. Ilgenfritz, and T. Suzuki, Phys. Rev. D **68,** 114504 (2003).

[48] P. Cea, L. Cosmai, and A. Papa, Phys. Rev. D **86,** 054501 (2012).

[49] J. R. Clem, J. Low Temp. Phys. **18,** 427 (1975).

[50] M. Falcioni, M. Paciello, G. Parisi, and B. Taglienti, Nucl. Phys. **B251,** 624 (1985).

[51] M. Albanese *et al.,* Phys. Lett. B **192,** 163 (1987).

[52] P. Skala, M. Faber, and M. Zach, Nucl. Phys. **B494,** 293 (1997).

[53] N. Cabibbo and E. Marinari, Phys. Lett. **119B,** 387 (1982).

[54] R. G. Edwards, U. M. Heller, and T. R. Klassen, Nucl. Phys. **B517,** 377 (1998).

[55] M. Caselle and P. Grinza, J. High Energy Phys. 11 (2012) 174.

[56] A. Shibata, K.-I. Kondo, S. Kato, and T. Shinohara, Phys. Rev. D **87,** 054011 (2013).

[57] A. Shibata, K.-I. Kondo, S. Kato, and T. Shinohara, *Proc. Sci.* LATTICE2013 (**2014**) 506 [arXiv:1403.3809].

[58] A. Shibata, K.-I. Kondo, S. Kato, and T. Shinohara, arXiv:1403.3888.

[59] P. Bicudo, M. Cardoso, and N. Cardoso, *Proc. Sci.* LATTICE2013 (**2014**) 495 [arXiv:1401.6008].